Communications on Applied Nonlinear Analysis
ISSN: 1074-133X
Vol 32 No. 10s (2025)

Mathematical Modeling and Analysis of the Amaranth Drying Curve: Evaluation of Functional Properties

[1]Giménez-López, Bruno César; [1]Ronceros Morales, Cristhian; [3]Cusi Palomino, Rosalio; [1]León-Castillo, Cesar Miguel; [1]Cuba Cornejo, Carmen Luz; [2]Giménez-Medina, Manuel Antonio, [4] García Agüiño, Oscar René.

1 Universidad Tecnológica del Perú, Ica, Perú.

2 Universidad Privada San Juan Bautista, Escuela Profesional de Ingeniería Agroindustrial, Ica, Perú.

3 Universidad Nacional San Luis Gonzaga de Ica, Perú.

4 Universidad Centroccidental Lisandro Alvarado, Decanato de Agronomía, Laboratorio de Tecnología II, Barquisimeto, Venezuela.

Article History:

Received: 12-01-2025

Revised: 15-02-2025

Accepted: 01-03-2025

Abstract:

Introduction: The use of mathematical models to understand the dehydration of amaranth improves the efficiency and quality of drying, benefiting costs, sustainability, and product innovation.

Objectives: The main objective was to validate different mathematical models that accurately describe the drying process, allowing the determination of the kinetic and thermodynamic parameters that govern it, as well as the physicochemical and functional characteristics of the resulting amaranth flour.

Methods: Amaranthus dubius seeds were cleaned, disinfected, cooked at 70°C for 30 minutes, and then dried at 60, 70, and 80°C in a tray dryer with controlled airflow. Dried samples were ground and sieved. Moisture content during drying was modeled using five mathematical models, Page, Midilli, Lewis, Logarithmic and the de Henderson y Pabis. The effective moisture diffusion coefficient and activation energy were determined using Fick's second law and the Arrhenius model. Functional properties such as water retention capacity, oil absorption capacity, and gelation capacity were evaluated using standard methods. Statistical analysis included ANOVA and Tukey's test with a significance level of $p < 0.05$.

Results: the Midilli model being the one that best adapted to the experimental curves, demonstrating precision in representing the drying curve of amaranth flour. On the other hand, lower moisture percentages (9.09 ± 0.15%) and water activity (0.45 ± 0.00) were found when the drying temperature was 80 °C, and the obtained flour showed a remarkable water retention capacity, while the emulsifying capacity showed its highest value in the flours obtained at 70 and 80°C. These findings underscore the importance of selecting the drying temperature properly in the production process of amaranth flour, as it can significantly influence its physical and functional properties, which in turn impacts its suitability as a functional ingredient for formulating various types of foods.

Conclusions: the results obtained in this study allowed us to conclude that the Midilli model was the one that best adapted to the experimental curves, demonstrating its precision in representing the drying behavior of amaranth flour. Furthermore, it was found that a drying temperature of 80 °C resulted in the lowest moisture content and water activity, which translates into greater product stability. The flour obtained at this temperature exhibited a remarkable water retention capacity, while the emulsifying capacity reached its highest

values in the flours dried at 70 and 80 °C. These findings highlight the importance of selecting an appropriate drying temperature during the production process, as it can significantly influence the physical and functional properties of amaranth flour, directly impacting its suitability as a functional ingredient in the formulation of various foods.

Keywords: Mathematical modeling; drying kinetics; Amaranth flour; Functional properties; drying temperature.

1. Introduction

Amaranth (*Amaranthus viridis* M.) is a nutrient-rich plant, primarily in volatile compounds [1]. This makes the drying stage critical in its processing, significantly impacting the quality and efficacy of foods with elevated nutritional levels [2]. Consequently, inefficient drying can lead to substantial nutrient losses and a significant increase in energy consumption, directly affecting production costs and the environment [1], [3].

To improve drying processes, mathematical models and the simulation of drying curves enable optimal process control and the production of high-quality products [4]. The development of robust mathematical models enables the integration of thermodynamic variables, mass and energy transfer kinetics, and the physical properties of the material, facilitating scenario simulation and the quantification of cause-effect relationships for data-driven decision-making [5]. These tools enhance operational efficiency and process sustainability by reducing energy consumption, preventing premature wear of drying equipment, and preserving final product quality [6], [7].

This is because mathematical models allow for the optimization of kinetic and thermodynamic parameters in the drying process [8]. For example, Silveira et al. [9], propose the Lewis linear model to describe drying kinetics, while Compaoré et al. [10], suggest a nonlinear model such as the Midilli model. On the other hand, Attkan et al. [11], and Revaskar et al. [12], argue that nonlinear models like the Page model or the modified Page model, respectively, better fit experimental drying curves. Other applied models include the convection model [13], the osmotic dehydration-freezing model [14], the microwave model [15], [16], and the fluidized bed model equipped with a heat pump dehumidifier [17], among others. However, all these models differ in how they express the relationship between drying rate and residual moisture.

Therefore, the purpose of this research is to determine the mathematical model that best fits the experimental drying curves of amaranth seeds at different drying temperatures and to evaluate its effect on the functional properties of Amaranthus viridis M., during processing and storage. This optimization aims to enhance the process from both an energy efficiency and product quality perspective, enriching the body of knowledge in agrifood process engineering. Additionally, it establishes foundations for future research in this field, opening new opportunities for technological advancement and innovation in food processing.

2. Objectives

The purpose of this research is to determine the mathematical model that best fits the experimental drying curves of amaranth seeds at different drying temperatures and to evaluate its effect on the functional properties of Amaranthus viridis M., during processing and storage. This optimization aims

to enhance the process from both an energy efficiency and product quality perspective, enriching the body of knowledge in agrifood process engineering. Additionally, it establishes foundations for future research in this field, opening new opportunities for technological advancement and innovation in food processing.

3. Methods

a) Raw Material

240 amaranth plants (Amaranthus dubius M.) were purchased from a supplier at the local market of Arenales in Ica, Peru, yielding 6345 g of seeds. These seeds were carefully washed and disinfected with 25 ppm sodium chloride solution. Subsequently, the seeds were filtered and cooked at 70°C for 30 minutes. After cooking, the Amaranthus dubius M., seeds were dried in an ESCO brand tray dryer (Model OFA-170-8), equipped with electrical heating elements. This equipment achieved a drying speed of 10 $m \cdot s^{-1}$ and maintained a constant flow of dry air at 3.0 ± 0.2 $m \cdot s^{-1}$, with a total load capacity of 5 kg. The drying temperatures used were 60, 70, and 80°C. The dimensionless moisture ratio (MR) was calculated according to the following equation (1):

$$MR = \frac{M_t - M_e}{M_0 - M_e} \quad (1)$$

Where Mt indicates the moisture content at time (t) until constant weight is reached, Me is the equilibrium moisture content, and M0 is the initial moisture content. Once the samples were completely dry, they were ground using a Corona® mill and then sieved through a 0.250 mm mesh. Subsequently, the samples were packed in polyethylene bags with airtight seals and stored under refrigeration at 5°C until the corresponding functional analyses were conducted.

b) Mathematical Models

In Table 1 shows five simplified mathematical models that explain the evolution of moisture content during the drying of *Amaranthus dubius* M., seeds.

Table 1. Mathematical models describing the drying processes of Amaranthus dubius M.

Model Name	Model equation	Nº
Page	$MR = exp(-kt^n)$	(2)
Midilli	$MR = a * exp(-kt^n) + (b * t)$	(3)
Lewis	$MR = exp(-kt)$	(4)
Logaritmo	$MR = a * exp(-kt) + c$	(5)
Henderson y Pabis	$MR = a * exp(-kt)$	(6)

Where a, b, c, k, and n represent the kinetic constants of the models, while MR is the moisture ratio.

c) Diffusion Coefficient, Activation Energy

The effective moisture diffusion coefficient (Deff), expressed in square meters per second (m^2.s-1), was calculated using Fick's second law of diffusion applied to different drying temperatures. This determination is based on the assumption that the temperature remains constant during the drying process, with no significant changes. For this calculation, the equation modeling the drying process was used:

$$-ln(MR) = \left(\frac{\pi^2 D_{eff}}{4L_0^2}\right)t - ln\left(\frac{8}{\pi}\right) \quad (7)$$

When analyzing the relationship between drying time (t) and moisture ratio (MR) of Amaranthus dubius M., seeds, and considering that their geometry resembles a slab (where L_0 represents half the thickness of the material and Deff is the measure of moisture's ability to diffuse through the material), the effective diffusion coefficient can be calculated from the slope (m) of the linear plot derived from Equation 7 can be used to calculate Deff.

$$\left(\frac{4mL_0^2}{\pi^2}\right) = D_{eff} \quad (8)$$

Considering that the Deff in foods exhibits a significantly temperature-dependent relationship with drying temperature, and its behavior aligns with the Arrhenius model, it is established that the relationship between Deff and drying air temperature (Ta) is accurately described by the Arrhenius model.

$$D_{eff} = D_0 exp^{\left[-\frac{Ea}{RT_a}\right]} \quad (9)$$

Where R is the universal gas constant (8.314 $J \cdot mol^{-1} \cdot K^{-1}$), E_a is the activation energy ($J \cdot K^{-1} \cdot mol^{-1}$), D_0 is the pre-exponential factor or initial diffusion constant ($m^2 \cdot s^{-1}$), and Ta is the absolute temperature (K). From the linearized Arrhenius equation, as shown in Equation 10, it is observed how Deff varies with the absolute temperature (Ta) measured in kelvin.

$$-ln(D_{eff}) = \left(\frac{Ea}{R}\right)\left(\frac{1}{Ta}\right) + lnD_0 \quad (10)$$

D_0 is calculated from the slope (m) and intercept (b), respectively, of the plot derived from Equation (10). Additionally, once Ea is known, it is possible to calculate the changes in enthalpy (ΔH), entropy (ΔS), and Gibbs free energy (ΔG) using the following equations:

$$\Delta H = E_a - RT \quad (11)$$

$$\Delta S = R\left(lnD_0 - ln\left(\frac{k_B}{h_p}\right) - lnT\right) \quad (12)$$

$$\Delta G = \Delta H - T\Delta S \quad (13)$$

Where, KB represents the Boltzmann constant (1.38×10^{-23} $J \cdot K^{-1}$), hp is the Planck constant (6.626×10^{-34} J·s), T is the absolute temperature measured in kelvin.

d) Functional Properties of Amaranth Flour

Water Retention Capacity

The water retention capacity (WRC) of Amaranthus dubius M., flour was determined at room temperature (28 ± 2°C) using the Onwuka method [18]. One gram (W_1) of the sample was poured into a centrifuge tube and weighed (W_2). Then, 10 mL of distilled water was added to the tube. The contents were mixed using an electric vortex mixer for 2 minutes and allowed to rest at room temperature (28 ± 2°C) for 30 minutes. The tubes were centrifuged at 3000 rpm for 10 minutes using a centrifuge

(FOUR Model CF-0202003). The supernatant liquid was drained at a 45° angle for 10 minutes. The remaining contents of the tube were then removed and weighed (W_3). The WRC was expressed as the percentage of water volume absorbed per sample weight, as shown in Equation (14).

$$WRC = \left(\frac{w_3 - w_2}{w_1}\right) x100\% \quad (14)$$

Where W_3 is the weight of the centrifuge tube plus the sample after centrifugation and decanting, W_2 is the weight of the tube plus the sample before centrifugation and W_1 is the weight of the sample.

Oil Absorption Capacity

The oil absorption capacity (OAC) of Amaranthus dubius M., flour was determined at room temperature (28 ± 2°C) using the Onwuka method [18]. One gram (W_1) of the sample was measured into a pre-weighed centrifuge tube (W_2). Then, 10 mL of soybean oil was added to the tube containing the sample. The mixture was blended for 60 seconds and allowed to rest at room temperature (28 ± 2°C) for 10 minutes. Subsequently, it was centrifuged at 3000 rpm for 30 minutes using the centrifuge (FOUR Model CF-0202003). The oil was carefully poured off, allowing it to drain at a 45° angle for 10 minutes, and the tubes were weighed (W_3). The OAC was calculated as the percentage of oil volume absorbed by the samples, as shown in Equation (15).

$$OAC = \left(\frac{w_3 - w_2}{w_1}\right) x100\% \quad (15)$$

Where W1 is the weight of the sample, W2 is the weight of the tube plus the sample before centrifugation and W3 is the weight of the tube plus the sample after centrifugation and decanting.

Gelation Capacity

The gelation capacity (GC) of Amaranthus dubius M., flour was determined using the Onwuka method [18]. Suspensions of amaranth flour at 2, 4, 6, 8, 10, 12, 14, 16, 18, 20, 22, and 30% (w.v-1) were prepared in 5 mL of distilled water and heated to 100°C for 1 hour in a water bath. The mixtures were then cooled in an ice-water bath at 1.0 ± 0.2°C for 1 hour. The minimum gelation concentration was assessed as the concentration at which all samples in the inverted tube did not slide. Gelation was defined as the lowest concentration at which the sample in the inverted tube did not fall or slide.

e) Statistical Analysis

The suitability of the proposed models for the drying kinetics of the two onion varieties was evaluated using statistical tests involving the sum of squared errors (SSE), calculated via Equation 16 and processed with Excel software. The lowest SSE values (≈0.0) were used as the criterion to select the model that best fit the experimental curve.

$$SSE = \frac{1}{N}\sum_{i=1}^{N}\left(MR_{e,i} - MR_{c,i}\right)^2 \quad (16)$$

In the equation (16), MRe,i represents the experimental moisture content, MRc,i is the calculated moisture content, i is the number of terms, and N is the number of data points. The results obtained for the functional properties were subjected to analysis of variance (ANOVA) to determine potential statistical differences between the properties of the flours produced under the three temperature

treatments (60°C, 70°C, and 80°C). If significant differences between means were observed, Tukey's test was applied, setting a significance level of $p < 0.05$.

4. Results

a) Drying Curves

Figure 1 shows the drying curves obtained experimentally for Amaranthus dubius M., at different drying temperatures 60, 70 and 80°C depending on the relative humidity (MR).

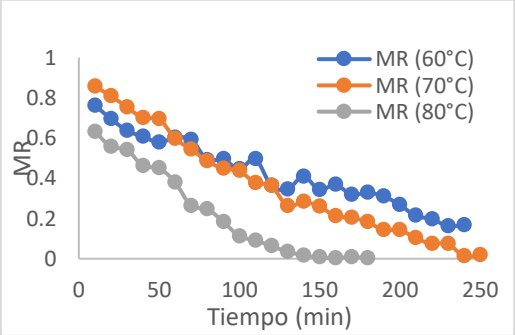

Figure 1. Dimensionless moisture content (MR) curves as a function of time, under three different drying temperatures: 60, 70 and 80 ºC for Amaranthus dubius.

Figure 1 reveals that during the drying of Amaranthus dubius M., increasing the air-drying temperature significantly reduces the relative humidity. It is also evident that equilibrium moisture content is reached more rapidly at a drying temperature of 80°C, achieving this state within 150 minutes.

Table 2. Empirical Models and Regressive Statistical Parameters of Amaranthus dubius M.

Model	T (˚C)	SMC	K	n	a	c	b
Lewis		0.134	7.9×10^{-3}				
Page		0.060	3.4×10^{-2}	0.5			
Henderson y Pabis	60	0.035	5.7×10^{-3}		0.69		
Logaritmo		0.028	3.5×10^{-3}		1.30	-0.543	
Midilli		0.021	1.5×10^{-5}	2.1×10^{-8}	0.70		-2.5×10^{-3}
Lewis		0.059	9.2×10^{-3}				
Page		0.045	5.4×10^{-3}	2.2			
Henderson y Pabis	70	0.055	9.9×10^{-3}		1.50		
Logaritmo		0.012	6.3×10^{-3}		1.60	-0.196	
Midilli		0.008	3.1×10^{-3}	1.6	1.21		-9.3×10^{-5}
Lewis		0.118	3.0×10^{-2}				
Page		0.117	3.6×10^{-2}	1.1			
Henderson y Pabis	80	0.098	1.7×10^{-2}		1.15		
Logaritmo		0.031	9.7×10^{-3}		1.36	-0.365	
Midilli		0.015	1.3×10^{-4}	2.0	0.83		-2.0×10^{-4}

When applying a one-way analysis of variance (ANOVA) with a 95% confidence level and Tukey's comparison test, it was determined that, at two of the studied drying temperatures, the Midilli model exhibited the lowest sum of squared errors (SSE).

Table 3. Results of Tukey's comparison test for different empirical models at a 95% confidence level for various drying temperatures of Amaranthus dubius M.

Modelo	Temperatura (^{0}C)	SSE
Lewis	60	0.134 ^{A}
Page		0.060 ^{B}
Henderson y Pabis		0.035 ^{C}
Logaritmo		0.028 ^{CD}
Midilli		0.021 ^{D}
Lewis	70	0.059 ^{A}
Page		0.055 ^{B}
Henderson y Pabis		0.045 ^{C}
Logaritmo		0.012 ^{D}
Midilli		0.008 ^{E}
Lewis	80	0.118 ^{A}
Page		0.117 ^{A}
Henderson y Pabis		0.098 ^{B}
Logaritmo		0.031 ^{C}
Midilli		0.015 ^{D}

When applying a one-way analysis of variance (ANOVA) with a 95% confidence level and Tukey's comparison test, it was determined that, at two of the studied drying temperatures, the Midilli model exhibited the lowest sum of squared errors (SSE). However, at 60°C, the results indicated no statistically significant differences between the Midilli model and the logarithmic model, as shown in the following table.

Table 3. Results of Tukey's comparison test for different empirical models at a 95% confidence level for various drying temperatures of Amaranthus dubius M.

Modelo	Temperatura (^{0}C)	SSE
Lewis	60	0.134 ^{A}
Page		0.060 ^{B}
Henderson y Pabis		0.035 ^{C}
Logaritmo		0.028 ^{CD}
Midilli		0.021 ^{D}
Lewis	70	0.059 ^{A}
Page		0.055 ^{B}
Henderson y Pabis		0.045 ^{C}
Logaritmo		0.012 ^{D}
Midilli		0.008 ^{E}
Lewis	80	0.118 ^{A}
Page		0.117 ^{A}
Henderson y Pabis		0.098 ^{B}
Logaritmo		0.031 ^{C}
Midilli		0.015 ^{D}

Note: Means that do not share a letter are significantly different.

b) Diffusion Coefficient of Amaranthus dubius

Fick's second law was applied to calculate the effective water diffusion coefficient (Deff), and Table 3 presents the results obtained for *Amaranthus dubius* M., at different drying temperatures. It was

observed that the Deff values for Amaranthus dubius M., increased as the drying temperature rose, ranging from 1.2×10^{-7} to 5.6×10^{-7} $m^2 \cdot s^{-1}$ within the 60–80°C temperature range.

Table 4. Effective diffusivity coefficient (Deff) for *Amaranthus dubius* M., at different drying temperatures (60, 70 and 80 ºC).

T (K)	D_{eff} ($m^2.s^{-1}$)
333.15	1.2×10^{-7}
343.15	3.2×10^{-7}
353.15	5.6×10^{-7}

c) Thermodynamic properties of *Amaranthus dubius* M.

The values found for the enthalpy differential (ΔH), entropy differential (ΔS), and Gibbs free energy are detailed in Table 5.

Table 5. Thermodynamic parameters for Amaranthus dubius M.

T (°C)	ΔH (kJ mol^{-1})	ΔS (kJ mol^{-1} K^{-1})	ΔG (kJ mol^{-1})
60	73.1	-249	156
70	73.0	-251	159
80	72.9	-247	160

d) Activation Energy

Understanding the activation energy (E_a) allows for the selection of optimal temperature and operating time during drying, and using the slope of the linearized Arrhenius equation, the E_a for Amaranthus dubius M., was calculated as 75.881 ± 0.012 $kJ \cdot mol^{-1}$.

e) Functional Properties of Amaranth Flours

Table 6 presents the functional properties of flours derived from Amaranthus dubius M. inflorescences subjected to three drying temperatures (60, 70, and 80°C).

Parámetros	Tratamientos		
	(60 ºC)	(70 ºC)	(80 ºC)
Capacidad de retención de agua ($mL.g^{-1}$)	6.3 ± 0.11^a	7.2 ± 0.57^a	$8,2 \pm 0,57^b$
Capacidad de absorción de aceite ($mL.g^{-1}$)	2.0 ± 0.20^a	1.7 ± 0.26^a	$1,8 \pm 0,10^a$
Capacidad gelificante (%)	No gelificó	No gelificó	No gelificó

Note: Averages within a row with the same letter do not present statistically significant differences (p value < 0.05) according to Tukey's statistical comparison test.

Statistically significant differences ($p < 0.05$) were observed between the treatments at 60°C and 70°C compared to the treatment at 80°C for drying Amaranthus dubius M. The higher water absorption in flour dried at 80°C may be attributed to the thermal treatment's impact on the flour's functional properties.

5. Discussion

a) Drying Curves

Figure 1 shows that during the drying process of Amaranthus dubius M., increasing the air-drying temperature significantly reduces the relative humidity. It is also observed that the equilibrium moisture content is reached much faster at a temperature of 80°C, achieving this state in just 150 minutes. The removal of the monolayer of adsorbed water molecules, which occurs in the final stage of drying, requires a large amount of energy, resulting in higher energy consumption during the process [19]. The observed trend of faster drying time reduction with increasing temperature aligns with findings from studies such as those by Avila et al., [20] on timbo leaves, Silva-Paz et al., [21] on muña, and Gasparin et al., [22] on Mentha × piperita leaves. This phenomenon can be explained by the structure of the dried portion of food products, which decisively influences the formation of a material-liquid complex. This complex determines the energy required to break the bond between water and the material's structure during drying [19].

The model proposed based on the results obtained matches the one proposed by Süfer et al., [16] as the most suitable for the investigated drying techniques. Revaskar et al., [12], however, recommended the Page model as the best descriptor of experimental curves when evaluated on onion slices and Lopes et al., [8] in blueberry the model with the best fit was that of Henderson and Pabis and the two-term exponential model. Other authors propose models distinct from linear or nonlinear approaches, such as Jafari et al., [17], who introduced a forward backpropagation neural network model using the Levenberg-Marquardt training algorithm.

b) Diffusion Coefficient of Amaranthus dubius

It was observed that the Deff values for *Amaranthus dubius* M., increased as the drying temperature rose, ranging from 1.2×10^{-7} to 5.6×10^{-7} $m^2 \cdot s^{-1}$ within the 60–80°C temperature range. These values align closely with those previously reported by Süfer et al., [16], who obtained diffusion coefficients between 1.962×10^{-9} and 1.372×10^{-8} $m^2 \cdot s^{-1}$ for convective drying, 9.8×10^{-9} to 1.7×10^{-8} $m^2 \cdot s^{-1}$ for vacuum drying (both processes conducted at 50–70°C), and 3.193×10^{-8} to 9.139×10^{-7} $m^2 \cdot s^{-1}$ for microwave drying. Similarly, Attkan et al., [11] reported effective moisture diffusivity values in onion slices ranging from 1.33×10^{-8} to 2.49×10^{-8} $m^2 \cdot s^{-1}$ using a low-humidity air-assisted hybrid solar dryer.

As observed, the values found for ΔH (enthalpy change) and ΔS (entropy change) are lower than those reported by Braga da Silva et al., [23]. On the other hand, the Gibbs free energy (ΔG) values mentioned by Silveira Dorneles et al., [9] for pretreated Piper aduncum leaves ranged between 108.955 and 113.889 $kJ \cdot mol^{-1}$, while for laurel leaves, the value was 53.038 $kJ \cdot mol^{-1}$—significantly higher than those found for onion [24].

c) Activation Energy

Understanding the activation energy (E_a) is essential for selecting the optimal temperature and operating time during the drying process. High E_a values indicate slow and prolonged drying, which can increase production costs. On the other hand, low E_a values result in rapid drying, but this may compromise product quality by damaging the material's structural layers [6].

By using the slope of the linearized Arrhenius equation, the E_a for Amaranthus dubius M. was calculated as 75.881 ± 0.012 kJ·mol^{-1}, which is considerably higher than the values reported by Süfer et al. [16] for *Allium cepa* L. These values ranged from 3.28 to 34.13 kJ·mol^{-1} for convective and vacuum drying, and from 2.25 to 6.08 W·kg^{-1} for microwave drying. These results confirm that the activation energy is independent of drying conditions [10].

d) Functional Properties of Amaranth Flours

Statistically significant differences ($p < 0.05$) were observed between the treatments at 60°C and 70°C compared to the treatment at 80°C for drying Amaranthus dubius M. The higher water absorption in flour dried at 80°C may be attributed to the thermal treatment's impact on the flour's functional properties. Studies have shown that heat treatments can increase water retention capacity and sucrose solvent retention capacity in flours, indicating enhanced protein hydration [25].

This property relates to the ability of proteins to hydrate, as proposed by Kalayan et al., [25] and is critical in food systems due to its effects on food flavor and texture [26]. Similarly, Yeung & Huang [27] suggest that minor structural changes in proteins through chemical modifications can improve specific functional properties required for food formulation.

Oil absorption capacity, as shown in Table 3, revealed no significant differences ($p > 0.05$) between samples subjected to different treatment temperatures. Oil absorption is linked to the number of non-polar side chains in proteins, which bind to hydrocarbon chains in fats [28]. This property is crucial for formulating bakery products, soups, and fried foods, as it relates to flavor retention and product tenderness [29]. As shown in Table 3, gelation capacity was not observed in amaranth flour suspensions.

The observed trend of faster drying time reduction with increasing temperature aligns with findings from studies such as those by Avila et al., [20] on timbo leaves, Silva-Paz et al., [21] on muña, and Gasparin et al., [22] on Mentha × piperita leaves. This phenomenon can be explained by the structure of the dried portion of food products, which decisively influences the formation of a material-liquid complex. This complex determines the energy required to break the bond between water and the material's structure during drying [19].

The model proposed based on the results obtained matches the one proposed by Süfer et al., [16] as the most suitable for the investigated drying techniques. Revaskar et al., [12], however, recommended the Page model as the best descriptor of experimental curves when evaluated on onion slices and Lopes et al., [8] in blueberry the model with the best fit was that of Henderson and Pabis and the two-term exponential model. Other authors propose models distinct from linear or nonlinear approaches, such as Jafari et al., [17], who introduced a forward backpropagation neural network model using the Levenberg-Marquardt training algorithm.

The Midilli model is the most suitable for representing the experimental data of the drying process of Amaranthus dubius M., regardless of variations in drying temperature. Increasing the temperature during drying significantly reduced the time required to remove moisture from Amaranthus dubius M., leading to a rise in the effective water diffusion coefficient. However, this temperature increase did not significantly affect the enthalpy differential, entropy, or Gibbs free energy, demonstrating that these thermodynamic properties remain relatively stable under the studied drying conditions. The functional properties of Amaranthus dubius M., flour are temperature-sensitive. The flour obtained at 80°C exhibited a higher water absorption capacity, while the emulsifying capacity peaked in samples treated at 70°C and 80°C. In contrast, oil absorption capacity showed no significant variations across treatments.

References

[1] I. A. J. Varalakshmi Thanikachalam, "Phytochemistry of amaranthus viridis: GC-MS analysis," Int J Curr Res Rev, vol. 13, no. 7, pp. 162–166, Apr. 2021, doi: 10.31782/IJCRR.2021.13713.

[2] A. K. Babu, G. Kumaresan, V. A. A. Raj, and R. Velraj, "Review of leaf drying: Mechanism and influencing parameters, drying methods, nutrient preservation, and mathematical models," Renewable and Sustainable Energy Reviews, vol. 90, pp. 536–556, Jul. 2018, doi: 10.1016/j.rser.2018.04.002.

[3] R. Chakraborty et al., "Fluidized Bed Drying of Wheatgrass: Effect of Temperature on Drying Kinetics, Proximate Composition, Functional Properties, and Antioxidant Activity," Foods, vol. 12, no. 8, Apr. 2023, doi: 10.3390/foods12081576.

[4] B. Lončar and L. Pezo, "Mathematical Modeling Approach and Simulation in Food Drying Applications," Foods, vol. 13, no. 3, p. 384, Jan. 2024, doi: 10.3390/foods13030384.

[5] F. Cao et al., "Energy consumption optimization model and system for the pellet drying process of straight grate," Drying Technology, vol. 42, no. 8, pp. 1357–1369, Jun. 2024, doi: 10.1080/07373937.2024.2356171.

[6] J. A. K. M. Fernando and A. D. U. S. Amarasinghe, "Drying kinetics and mathematical modeling of hot air drying of coconut coir pith," Springerplus, vol. 5, no. 1, Dec. 2016, doi: 10.1186/s40064-016-2387-y.

[7] R. Lemus-Mondaca, A. Vega-Gálvez, N. O. Moraga, and S. Astudillo, "Dehydration of Stevia rebaudiana Bertoni Leaves: Kinetics, Modeling and Energy Features," J Food Process Preserv, vol. 39, no. 5, pp. 508–520, Oct. 2015, doi: 10.1111/jfpp.12256.

[8] S. Lopes et al., "Mathematical Modeling of a Sustainable Dewatering Process for Blueberries and Raspberries Preservation," 2024, pp. 139–151. doi: 10.1007/978-3-031-54394-4_12.

[9] L. do N. Silveira Dorneles et al., "Effect of air temperature and velocity on drying kinetics and essential oil composition of Piper umbellatum L. leaves," Ind Crops Prod, vol. 142, p. 111846, Dec. 2019, doi: 10.1016/j.indcrop.2019.111846.

[10] A. Compaoré et al., "Convective drying of onion: modeling of drying kinetics parameters," J Food Sci Technol, vol. 56, no. 7, pp. 3347–3354, Jul. 2019, doi: 10.1007/s13197-019-03817-3.

[11] A. Attkan, M. Alam, A. Raleng, and Y. K. Yadav, "Drying Kinetics of Onion (Allium cepa L.) Slices using Low-humidity Air-assisted Hybrid Solar Dryer," Journal of Agricultural Engineering (India), vol. 58, no. 3, 2021, doi: 10.52151/jae2021581.1750.

[12] V. A. Revaskar, P. S. Pisalkar, P. B. Pathare, and G. P. Sharma, "Dehydration kinetics of onion slices in osmotic and air convective drying process," Res. Agr. Eng., vol. 60, no. 3, pp. 92–99, 2014, doi: 10.17221/22/2012-RAE.

[13] M. Przeor et al., "Air-drying temperature changes the content of the phenolic acids and flavonols in white mulberry (Morus alba L.) leaves," Ciência Rural, vol. 49, no. 11, 2019, doi: 10.1590/0103-8478cr20190489.

[14] D. Bosco, L. A. Roche, P. A. Della Rocca, and R. H. Mascheroni, "Osmodehidrocongelación de batata fortifcada con Zinc y Calcio," INNOTEC, vol. 15, Jun. 2018, doi: 10.26461/15.05.

[15] Y. K. Khodja, F. Dahmoune, M. Bachir bey, K. Madani, and B. Khettal, "Conventional method and microwave drying kinetics of Laurus nobilis leaves: effects on phenolic compounds and antioxidant activity," Brazilian Journal of Food Technology, vol. 23, 2020, doi: 10.1590/1981-6723.21419.

[16] Ö. Süfer, S. Sezer, and H. Demir, "Thin layer mathematical modeling of convective, vacuum and microwave drying of intact and brined onion slices," J Food Process Preserv, vol. 41, no. 6, p. e13239, Dec. 2017, doi: 10.1111/jfpp.13239.

[17] S. M. Jafari, M. Ganje, D. Dehnad, and V. Ghanbari, "Mathematical, Fuzzy Logic and Artificial Neural Network Modeling Techniques to Predict Drying Kinetics of Onion," J Food Process Preserv, vol. 40, no. 2, pp. 329–339, Apr. 2016, doi: 10.1111/jfpp.12610.

[18] G. I. Onwuka, Food Analysis and Instrumentation: Theory and Practice. Napthali Prints, 2005.

[19] J. Safarov, A. Khujakulov, S. Sultanova, U. Khujakulov, and S. Verma, "Research on energy efficient kinetics of drying raw material," in E3S Web of Conferences, EDP Sciences, Dec. 2020. doi: 10.1051/e3sconf/202021601093.

[20] W. Avila, I. A. Pordeus, S. M. Paiva, and C. C. . Martins, "Breast and Bottle Feeding as Risk Factors for Dental Caries: A Systematic Review and Meta-Analysis," PLoS One, vol. 10, no. 11, 2015, doi: 10.1371/journal.pone.0142922.

[21] R. J. Silva-Paz, D. K. Mateo-Mendoza, and A. Eccoña-Sota, "Mathematical Modelling of Muña Leaf Drying (Minthostachys mollis) for Determination of the Diffusion Coefficient, Enthalpy, and Gibbs Free Energy," ChemEngineering, vol. 7, no. 3, Jun. 2023, doi: 10.3390/chemengineering7030049.

[22] P. P. Gasparin, D. Christ, and S. R. M. Coelho, "Drying of Mentha piperita leaves on a fixed bed at different temperatures and air velocities," REVISTA CIÊNCIA AGRONÔMICA, vol. 48, no. 2, 2017, doi: 10.5935/1806-6690.20170028.

[23] N. C. Braga da Silva, S. G. Ferreira dos Santos, D. Pereira da Silva, I. L. Silva, and R. Souza Rodovalho, "Drying kinetics and thermodynamic properties of boldoleaves (Plectranthus barbatus Andrews)," Jaboticabal, vol. 47, no. 1, pp. 1–7, 2019, doi: http://dx.doi.org/10.15361/1984-5529.2019v47n1p1-7.

[24] W. D. Quequeto et al., "Mathematical Modeling of Thin-Layer Drying Kinetics of Piper aduncum L. Leaves," Journal of Agricultural Science, vol. 11, no. 8, p. 225, Jun. 2019, doi: 10.5539/jas.v11n8p225.

[25] J. Kalayan, A. Chakravorty, J. Warwicker, and R. H. Henchman, "Total free energy analysis of fully hydrated proteins," Proteins: Structure, Function and Bioinformatics, vol. 91, no. 1, pp. 74–90, Jan. 2023, doi: 10.1002/prot.26411.

[26] J. A. K. M. Fernando and A. D. U. S. Amarasinghe, "Drying kinetics and mathematical modeling of hot air drying of coconut coir pith," Springerplus, vol. 5, no. 1, p. 807, Dec. 2016, doi: 10.1186/s40064-016-2387-y.

[27] C. K. Yeung and S. C. Huang, "Effects of Food Proteins on Sensory and Physico-Chemical Properties of Emulsified Pork Meatballs," Journal of Food and Nutrition Research, vol. 6, no. 1, pp. 8–12, Dec. 2017, doi: 10.12691/jfnr-6-1-2.

[28] H. Yu, L. Qin, and J. Zhou, "Effect of Oil Polarity on the Protein Adsorption at Oil–Water Interfaces," Langmuir, vol. 39, no. 30, pp. 10701–10710, Aug. 2023, doi: 10.1021/acs.langmuir.3c01541.

[29] A. Goins and S. Griffin, "Methodological inconsistencies in novel plant protein functional properties, and improvements for water absorption capacity determinations," in Proceedings of 2022 AOCS Annual Meeting & Expo, American Oil Chemists' Society (AOCS), Sep. 2022. doi: 10.21748/ITJD9802.